esa

ECOSPHERE

Intra- and inter-annual variation in gray whale body condition on a foraging ground

Leila Soledade Lemos[1,†] Jonathan D. Burnett[2] Todd E. Chandler,[1] James L. Sumich[3] and Leigh G. Torres[1]

[1]*Geospatial Ecology of Marine Megafauna Lab, Marine Mammal Institute, Fisheries and Wildlife Department, Oregon State University, Corvallis, Oregon 97331 USA*
[2]*Aerial Information Systems Laboratory, Forest Engineering, Resources and Management Department, Oregon State University, Corvallis, Oregon 97331 USA*
[3]*Fisheries and Wildlife Department, Oregon State University, Corvallis, Oregon 97331 USA*

Citation: Soledade Lemos, L., J. D. Burnett, T. E. Chandler, J. L. Sumich, and L. G. Torres. 2020. Intra- and inter-annual variation in gray whale body condition on a foraging ground. Ecosphere 11(4):e03094. 10.1002/ecs2.3094

Abstract. Baleen whales store energy gained on foraging grounds to support reproduction and other metabolic needs while fasting for long periods during migration. Whale body condition can be used to monitor foraging success, and thus better understand and anticipate individual- and population-level trends in reproduction and survival. We assessed the body condition of eastern North Pacific gray whales (*Eschrichtius robustus*) on their foraging grounds along the Oregon coast, USA, from June to October of three consecutive years (2016–2018). We used drone photogrammetry and applied the body area index (BAI) to measure and compare whale body condition, which is a continuous, unitless metric similar to the body mass index in humans. A total of 289 drone flights were carried out over 106 photo-identified whales, which were grouped into demographic units by sex, maturity, and female reproductive status. Calves and pregnant females displayed the highest BAIs, followed by resting females, mature males, and, finally, lactating females, reflecting the significant energetic demands on reproductive females. In all three years, gray whale body condition improved with the progression of feeding seasons, demonstrating the accumulation of body energy reserves on the foraging grounds. Yet, body condition was significantly better in 2016 than in 2017 and 2018 when overall body depletion was observed, indicating a difference in prey availability and/or quality between years. We analyzed local upwelling patterns between 2013 and 2018 as an oceanographic proxy for prey and determined significantly greater upwelling between 2013 and 2015 than low upwelling years between 2016 and 2018. We hypothesize that these upwelling patterns created ecosystem shifts in primary productivity and zooplankton prey of gray whales, causing carry-over effects between foraging success and body condition in subsequent years. This study demonstrates the value of monitoring whale body condition to better understand temporal variation in foraging success, and potentially detect and describe the causes of anomalous changes in whale population health, such as the 2019 gray whale mortality event.

Key words: baleen whale; body area index; body condition; bottom-up trophic cascades; carry-over effects; drone; morphometrics; Oregon; USA; photogrammetry; unmanned aerial systems; upwelling.

Received 17 September 2019; revised 29 December 2019; accepted 7 January 2020; final version received 13 February 2020. Corresponding Editor: Hunter S. Lenihan.

† **E-mail:** leslemos@hotmail.com

Introduction

Tight links exist between ecosystem productivity, trophic pathways, and the health and viability of animal populations (Hunter 1978, Sinclair and Krebs 2002). In both terrestrial and marine ecosystems, grazer and predator populations are dependent on bottom-up trophic

cascades based on primary productivity (Sinclair and Krebs 2002, Benoit-Bird and McManus 2012). Therefore, environmental perturbations that disrupt a predictable source of prey availability could compromise a population's viability (Williams et al. 2013, Seyboth et al. 2016, Thompson et al. 2018). While certain animal populations may have evolved resiliency to periods of low prey availability (Nattrass and Lusseau 2016), cumulative prey shortages can cause poor body condition, health implications, and ultimately population declines (Acevedo-Whitehouse and Duffus 2009, Tollefson et al. 2010). Hence, population management can benefit from understanding variation in body condition of animals, as related to normal life history phases such as reproduction and growth, and in response to environmental conditions (National Academies of Sciences 2017). Monitoring individual- and population-level body condition can illuminate population health and associated factors, and the limits of population resilience to food limitations.

Marine ecosystems are particularly dynamic, both spatially and temporally, due to multiple oceanographic forces that influence various trophic pathways in the food web, from plankton to whales (Cury et al. 2008, Heymans et al. 2014). As large, long-lived, migratory marine animals, baleen whales are capital breeders that rely on energy storage acquired on feeding grounds to finance the costs of reproduction and fasting periods (Lockyer 1987*b*, Kasuya 1995). Thus, a successful feeding season is critical to gain energy stores to support their metabolic needs and reproductive success. For instance, it is estimated that female minke whales (*Balaenoptera acutorostrata*) investing in reproduction must increase their body weight by 65% to sustain the high energetic demands required by gestation and lactation (Lockyer 1981).

An unproductive foraging season resulting in low individual fat reserves may affect future reproductive performance and survival in subsequent seasons, a phenomenon known as the carry-over effect (Lockyer 1986, Harrison et al. 2011). Short-term energetic balance disruptions in whales with large reserves may lead to only marginal effects, but persistent poor foraging may profoundly affect individual fitness (New et al. 2013). Cumulative poor foraging could trigger a downstream process that leads to adverse effects on individual whale body condition, fecundity, reproduction, and survival (Lockyer 1986, Thomas 1990, Perryman et al. 2002, Harrison et al. 2011, Braithwaite et al. 2015*b*). For instance, the resting intervals of female fin whales (*Balaenoptera physalus*) following birth events may be longer if prey availability is insufficient during the foraging season (Lockyer 1986). Additionally, a female gray whale (*Eschrichtius robustus*) bioenergetics model described the energy requirements for a two-year reproductive cycle (Villegas-Amtmann et al. 2015) and determined that an annual energy loss of (1) 4% would result in a pregnant female to lose her calf; (2) 30–35% would prevent females to reproduce; (3) 37% would cause the lactating female to wean her calf at a lower mass; and (4) 40–42% would prevent females to survive. Thus, foraging success impacts calving intervals and rates, and calf and mother body condition and survival, all of which affect population growth rates (Villegas-Amtmann et al. 2015, Braithwaite et al. 2015*a*).

Innovative methods have been applied to study whale body condition and document variation relative to intrinsic (e.g., reproductive state; Perryman and Lynn 2002, Christiansen et al. 2016), environmental (Bradford et al. 2012, Williams et al. 2013), and anthropogenic (e.g., entanglement in fishing gear; Pettis et al. 2017) factors. Previous studies of whale body condition used whaling data (Lockyer 1986, 1987*a*, Christiansen et al. 2013) or photogrammetry of aerial images captured from airplanes (Best and Ruther 1992, Perryman and Lynn 2002, Miller et al. 2012) and, more recently, from unmanned aerial systems (UAS; drone; Christiansen et al. 2016, Durban et al. 2016, Burnett et al. 2018). While these studies did not monitor temporal trends in individual body condition due to logistical limits of replicate data acquisition, other studies have examined individual variation of body condition over time on a breeding ground using drone photogrammetry (Christiansen et al. 2018) and on a foraging ground through qualitative categorization of whale fat deposits in photographs (Pettis et al. 2004, Bradford et al. 2012). However, quantitative aerial photogrammetry methods have not yet been applied to assess individual- and population-level changes in whale body condition over a foraging season, which is critical to

understanding how whales respond to, and tolerate, changes in prey availability and quality.

In this study, we use drones to repeatedly sample gray whale body condition while on their foraging grounds along the Oregon coast, USA, during three consecutive years. Through analyses of these replicate data, we describe body condition variation relative to demographic unit, time, and environmental conditions, at both the individual level and aggregated population level, adding to the understanding of gray whale bioenergetics provided by previous studies (e.g., Rice and Wolman 1971, Perryman and Lynn 2002, Bradford et al. 2012, Villegas-Amtmann et al. 2015).

Eastern North Pacific (ENP) gray whales conduct one of the longest migrations of any mammal, as they reach up to 20,000 km round trip every year between their breeding grounds in Baja California, Mexico, and feeding grounds in the Bering and Chukchi seas, off the coast of Alaska, United States (Jones and Swartz 2002, Sumich 2014). A subset of this population, known as the Pacific Coast Feeding Group (PCFG), do not complete the full migration (Calambokidis et al. 2002, Lang et al. 2014). This group of ~250 individuals feed during summer and fall along the coast from northern California through southeastern Alaska, including the Oregon coast (Calambokidis et al. 2012, Weller et al. 2013). Possible explanations for this truncated migration are energetic savings of a shorter travel distance, leading to a longer foraging period, and efficient prey availability due to abundant food sources, such as mysid aggregations (*Holmesimysis sculpta*; Newell and Cowles 2006).

The development of drone-based whale photogrammetry methods facilitates easier, cheaper, and safer collection of replicate aerial whale images in a noninvasive fashion (Christiansen et al. 2016, Smith et al. 2016, Burnett et al. 2018) than previously attainable. We implement the quantitative and continuous metric of whale body area index (BAI) developed by Burnett et al. (2018) to assess PCFG gray whale body condition. The BAI allows comparative assessment of whale body condition between time steps, subgroups (e.g., by sex), and within individual to monitor and describe relative foraging success and health. The objectives of this study are to (1) examine intra- and inter-annual PCFG gray whale body condition variation during three consecutive foraging seasons; (2) describe how gray whale body condition varies with respect to demographic units; and (3) explore possible associations between gray whale body condition variability and oceanographic conditions.

Our study is particularly relevant in light of the 2019 unusual mortality event of ENP gray whales with many emaciated whales found stranded along the west coasts of Mexico, the United States, and Canada since January 2019 (NOAA 2019). Environmental anomalies and elevated intraspecific competition due to limits on carrying capacity are hypothesized causes of these mortalities, with both mechanisms causing low prey availability and hence depleted whale body condition. Our work establishes a baseline of gray whale body condition during the foraging season and by demographic unit, which may be used to identify trends, anomalies, and possible causes of mortality events. Using the concept of carry-over effects, we examine possible links between body condition and environmental variability, which elucidates drivers of whale bioenergetics and can inform population management.

Methods

Study area

This study was performed on two gray whale foraging areas along the coast of Oregon, USA: Port Orford (42°44′59″ N, 124°29′53″ W), in southern Oregon, and Newport (44°38′13″ N, 124°03′08″ W), in central Oregon. The study sites are ~180 km apart with photographically documented exchange of individual gray whales between areas within and between foraging seasons (L. Torres, *unpublished data*). The two sites are environmentally similar, comprising rocky nearshore environments, with the presence of patchy kelp habitats, and similar zooplankton communities (L. Torres, *unpublished data*).

Sampling methods

A small research vessel (a 5.4-m rigid-hulled inflatable boat) was used to locate gray whales and collect individual data during three feeding seasons between June and October of 2016, 2017, and 2018. Sampling was conducted in both study sites in the first two years and only in Newport in the last year, due to logistics. During whale

encounters, photographs of the left-hand side, right-hand side, and the fluke of each individual were obtained for photo-identification by using two cameras (Canon EOS 7D and Canon EOS 70D) simultaneously. In addition, the number of sighted whales and calf presence were recorded. Whale fecal samples were also collected opportunistically using a 300-μm sampling net (subsequently placed on ice until stored in a −20°C freezer), which enabled genetic sex determination.

When the whale behaved naturally during observation (i.e., no behavioral changes due to the presence of the research vessel) and weather conditions were appropriate, an UAS was launched from the vessel to conduct whale overflights and record videos during surfacing events. Three different drones were used during this study. A DJI Phantom 3 Pro was used in 2016, and a Phantom 4 was used in 2017. Both of these aircrafts included a camera with 3.61-mm focal length and pixel size (i.e., pitch) of approximately 0.0015 mm (at 4000 × 3000 image resolution). In 2018, a DJI Phantom 4 Pro was used, with 8.8-mm focal length camera and pixel size of approximately 0.0033 mm (at 4000 × 3000 image resolution). All aircrafts were remotely controlled using an Apple iPad Mini 4 tablet with the DJI Go 4 app.

Collection of whale photogrammetry data using the drone followed protocols described by Burnett et al. (2018). In short, the drone hovered above the whale, at a minimum altitude of 25 m. Whales were recorded while centered in the field of view and with the camera pointing straight down at the whale (i.e., nadir). Video metadata at 1-s intervals provided information on geolocation and altitude relative to initialization height, which was consistent throughout the study (1.0 m) and compensated for in the photogrammetry analysis. A calibration object of 1.0 m in length was centered in the frame of the drone camera during the beginning of all flights and recorded from 10 to 40 m of altitude for correction of barometric altimeter errors during postprocessing. All overflown whales were simultaneously photographed from the boat to confirm individual identification. Whale behavior was also monitored to assess changes in response due to the drone presence.

Analysis methods

Photo-identification.—Gray whale photo-identification was conducted using Adobe Bridge (version 8.0.1.282; Adobe Systems, San Jose, CA, USA) by visually assessing unique skin pigmentation and marks (e.g., scars) on the left-hand side, right-hand side, and fluke that are stable through time and identify distinct individuals (Hammond et al. 1990). Photograph quality was first assessed to ensure images were in-focus, well lit, and not affected by glare, angle, or distance (Darling 1984, Hammond et al. 1990). Images of each identified whale were compared with long-term (>30 yr) gray whale photo-id catalogs (held by the Marine Mammal Institute at Oregon State University, and by Cascadia Research Collective, Olympia, Washington, USA) in order to obtain sighting histories, which provided information on the whale's minimum age estimate based on date of first sighting, and sex based on previous genetic analysis of collected tissue samples (Lang et al. 2014). When sex information was not available, genetic analyses were performed on fecal samples collected from the individual whale, if available (see Appendix S1 for fecal genetic analysis methods).

Assignment to demographic unit.—Each individual whale was assigned into a demographic unit based on sex (male or female), maturity (immature, calves and juveniles; or mature, adults), and female reproductive status (resting, pregnant, lactating, and postweaning). It was assumed that (1) small whales (<8 m in length) swimming in close association with a large whale (>11 m in length) were calves (Perryman and Lynn 2002) and that the large whale was a lactating female mother, (2) a lactating female was a pregnant female in the previous year, and (3) a lactating female became a postweaning female when the calf was not associated with the mother in the same year. Resting females represent mature females that were not pregnant or lactating in the analysis year. Sexual maturity occurs at different ages and lengths in female and male gray whales (Zimushko 1969, Zimushko and Ivashin 1980). In females, it is attained between 8 and 12 yr, and at approximately 12 m. In males, sexual maturity is reached at 6–8 yr and at around 11.5 m. To obtain confidence in individual maturity classification, 8 and 12 yr of minimum age were applied as maturity age cutoffs for males and females,

respectively. Individuals at a length range between 10 and 12 m of unknown sex or age were classified as undetermined.

Photogrammetry.—Drone videos were viewed using the VLC Media Player software (version 2.2.8; VideoLAN, Paris, France.). Full-resolution frames of the whale during surfacing events were extracted using the snapshot function. We aimed to extract five images of each individual per flight, but this was not always possible due to non-ideal whale body positions and/or quality of the image. Once images were extracted, image quality was assessed and categorized as either good or poor, according to attributes relative to the whale body position (body straightness and body arching), camera focus, and environmental conditions (glare, water splash, and water turbidity; Appendix S2: Table S1, Fig. S1). If the image was not in-focus, the whale's body was bending or arched, or if any of the environmental factors masked >25% of one side of a body contour, the image was classified as poor and excluded from the analysis. (Photogrammetry analysis methods apply a best-fit parabola to analyst-defined points along the body edge contour, allowing for some gaps in edge definition by the analyst; see *Methods* below and Burnett et al. 2018.) Five images of the calibration object, at different altitudes, were also extracted from each drone video.

Images of calibration objects and whales assessed as good quality were, respectively, measured using the whale calibration object measurement and whale measurements programs in MATLAB (version 9.3.0.7; MathWorks, Natick, MA, USA) developed by Burnett et al. (2018). Using these programs, the analyst measured a single length value of the calibration object and a series of measurements of each whale image, which produced an output table containing 10 whale morphometric attributes (Table 1, Fig. 1) for each image. Morphometric attributes included common morphometrics (whale length, WL, and width, MW; Perryman and Lynn 2002), and a series of width measurements at different body length percentage points between 20% and 60% (W20–W60), to which the program fits parabolas along the body edges of these 20–60% points. According to Koopman (1998), head, fins, and fluke of cetaceans are not used as energy reservoirs. Therefore, body condition assessments were limited to between 20% and 60% of the body length where body shape is more likely to vary with energy reserves. Additional morphometrics produced are the manual width (MW, widest width measured manually), the optimized width (OW, point on parabola nearest MW), and the surface area (SA) between the two fitted parabolas.

Morphometric attributes were measured in pixels and converted to meters via ground sampling distance (GSD, i.e., ground distance of one pixel), assuming that the aircraft altitude above sea level (ASL) was zero (Burnett et al. 2018). Burnett et al. (2018) applied a GSD correction model by calculating the empirical GSD (eGSD, calibration object length in meters/calibration object length in pixels) and regressing eGSD on reported altitude. This model outputs a corrected GSD and accounts for systematic errors in altimeter observations (which propagate into GSD). The program also incorporates lens distortion corrections for each of the three drone cameras used in this study.

Using the whale quantitative analysis program (Burnett et al. 2018) in R (version 3.5.0; R Core Team 2019), measurement data of multiple images of the same whale were grouped by date, flight, and sighting to produce summarized measurement data, including BAI values and error estimates based on the measurements (Table 1; Fig. 1). To minimize the impact of measurement error, a threshold of 5% was applied for both WL and BAI coefficients of variance (CV). Any image

Table 1. Morphometric attributes calculated for whale photogrammetry analysis.

Attribute	Parameter	Description
1	FW	Fluke width, tip to tip fluke width
2	WL	Whale length, rostrum to notch in tail
3	W20	Width at 20% of WL from rostrum
4	W30	Width at 30% of WL from rostrum
5	W40	Width at 40% of WL from rostrum
6	W50	Width at 50% of WL from rostrum
7	W60	Width at 60% of WL from rostrum
8	MW	Manual width, manual measurement of width at widest point
9	OW	Optimized width, width at point on parabola nearest MW
10	SA	Surface area between 20% and 60% of WL
11	BAI	Body area index

Note: Modified from Burnett et al. (2018).

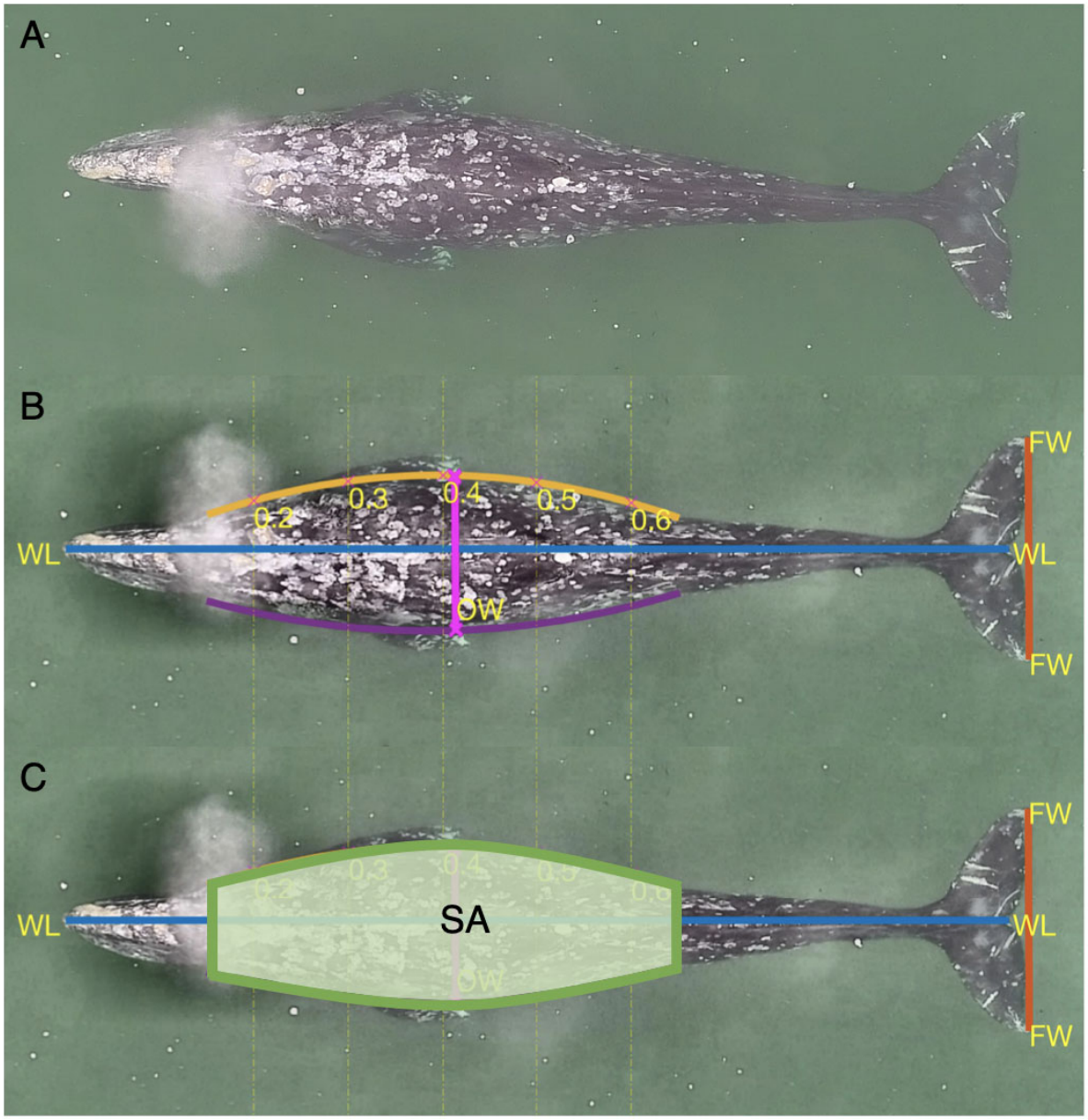

Fig. 1. Example surface image of a gray whale extracted from drone video and the morphometric measurements calculated during photogrammetry analysis using methods and programs developed by Burnett et al. (2018). (A) Extracted image of a whale at a surfacing event. (B) Measurements calculated: WL, whale length; FW, fluke width; OW, optimized width. 0.2–0.6: body proportion points, and parabolas (orange and purple lines) fit to the perimeter curves of the body based on location of 0.2–0.6 body percentage points. (C) Body surface area (SA) based on parabolas, from which the body area index (BAI) is calculated.

causing a CV to be higher than 5% was excluded from the final analysis.

BAI is similar to the body mass index (BMI) used to evaluate human health because both are unitless and scale-invariant metrics of body condition. BAI was developed based on the BMI formula (mass (Kg)/height $(m)^2$; Gallagher et al. 1996) by using SA as a surrogate for body mass

(Burnett et al. 2018) and calculated using the following equation:

$$\text{BAI} = \frac{\text{SA}}{(0.4 \times \text{WL})^2} \times 100.$$

Whale length (WL) is multiplied by 0.4 because SA is only captured across 40% of WL (between 20% and 60% body length). The final multiplication by 100 allows for a whole number BAI value.

An advantage of the BAI assessment of whale body condition is its scale invariance and independence of body length, which enables comparisons over time of body condition within and among individuals regardless of different body lengths (i.e., calves:adults or males:females). In addition, BAI is not influenced by scaling errors between pixels and metric units that may arise during photogrammetry efforts if altitude is uncertain. For instance, we encountered inaccurate altitude values in our 2016 data due to high flight speeds over the calibration board. (The flight speed was adjusted in the following years.) Consequently, absolute length and width values are not accurate from 2016, and only values from 2017 and 2018 are reported. However, since BAI is a unitless metric and is not affected by scaling errors, BAI values remain accurate and comparable between all years, including 2016. To verify the resilience of BAI values, we applied a linear regression to compare BAI values calculated from raw pixel values and from scaled metric values from the same whale images captured in 2017 and 2018.

Upwelling index.—In Oregon, coastal upwelling occurs annually, from April to September, bringing nutrient-rich water to the surface and fueling seasonal primary production (Mooers et al. 1976, Harvey et al. 2018, Peterson et al. 2018). This upwelling season overlaps with gray whale presence in the study area and may be a significant driver of the availability of their zooplankton prey. Although no study has directly addressed this hypothesis, other studies in the California Current System (CCS) have found significant correlations between upwelling strength and zooplankton biodiversity and abundance, including copepod and krill species (Thompson et al. 2018). Thus, we investigated possible correlations between population-level whale body condition and oceanographic conditions by extracting upwelling index data from 6-hourly composites of one-degree Fleet Numerical Meteorology and Oceanography Center sea level pressure at the location closest to our main study site (Newport, OR, −45° N, 125° W). We sampled the data during the study period (2016–2018) and the previous three years (2013–2015) to evaluate possible carry-over effects on gray whale body condition. The cumulative upwelling index sum (CUI) was computed by first calculating the daily upwelling index means from the six-hourly data, and then calculating the cumulative sum of daily upwelling index means for each day based on the days since 1 January of that year. Hence, CUI provides an estimate of the net influence of upwelling strength on the ecosystem as a proxy of variation in productivity throughout the year (Bograd et al. 2009).

In order to compare upwelling conditions prior to the 2019 gray whale mortality event and a previous mortality event during 1999–2000 (Le Boeuf et al. 2000, Moore et al. 2001), we also conducted the CUI analysis for the period of 1993–1998.

Statistical methods

The Shapiro-Wilk normality test verified the normal distribution of all variables assessed. All statistical tests were conducted in R (version 3.5.0; R Core Team 2019).

To assess the influence of multiple factors on changes in BAI while also accounting for individual replication, a linear mixed model (LMM) was applied, using the lme4 package in R (Bates et al. 2015). The influence of the following predictor variables on the response variable BAI was tested: demographic unit, day, month, year, and study site (Newport or Port Orford). All models included the whale identification as a random effect to account for pseudoreplication. Model selection was based on Akaike's information criterion (AIC; Burnham et al. 2011). Nonsignificant variables were excluded to use the most parsimonious model. To evaluate the LMM fit, marginal R^2 (R^2_m, variance explained by fixed effects) and conditional R^2 (R^2_c, variance explained by both fixed and random effects, or the entire model) were assessed using the MuMIn package (Nakagawa and Schielzeth 2013, Barto 2018). The P values and F statistics were obtained using the

lmerTest package (Kuznetsova et al. 2017). A pairwise analysis of estimated marginal means was conducted to compare significant fixed effects, using the emmeans package in R (Lenth 2019). In addition, a generalized linear model (GLM) was conducted to determine the effects of month and year on CUI, which followed a Gaussian distribution. For all tests, a P value of 0.05 level of significance was considered.

Linear regressions were also conducted using the lm function in R to describe (1) the trend in gray whale BAI change over the three seasons; (2) the relationship between gray whale body length (WL) and optimized width (OW); and (3) the resilience of BAI values calculated by raw pixel values relative to scaled metric values for whales measured in 2017 and 2018.

Photogrammetry analysis of good quality images from 2016 was conducted by two analysts, and a t-test was conducted to assess potential bias in calibration object and whale measurements between analysts. As no statistically significant difference between observer measurements was found ($t = 0.829$, $P = 0.41$), only one observer (LSL) continued measuring the whales and calibration boards in the following seasons.

Results

A total of 171 whales were photo-identified during our study period from 2016 to 2018, comprising 40 females, 40 males, and 91 unsexed individuals. Fifteen of the sexed individuals were determined by fecal genetic analyses (eight females and seven males). Eleven of the unsexed individuals were calves sighted along with their mothers (2016, $n = 9$; 2017, $n = 1$; and 2018, $n = 1$).

A total of 289 drone flights (2016, $n = 76$; 2017, $n = 113$; and 2018, $n = 81$) were performed over 62% of the identified whales ($n = 106$). Sixteen unique gray whales were flown over in all the three feeding seasons, 25 in two seasons and 65 only in one season. However, only 272 drone observations of 104 individuals were analyzed after image quality assessment, with varying sample sizes by year and demographic unit (Table 2).

We noted no behavioral response of whales to the drone overflights, either in the field or during video review.

Whale lengths and widths

For the combined 2017 and 2018 dataset, mean WL ± standard deviation (SD) and mean OW ± SD for mature females ($n = 29$) were 12.43 m ± 0.90 (range 10.23–14.12) and 2.13 m ± 0.23 (range 1.63–2.61), respectively, while mature male ($n = 29$) values were 11.59 m ± 0.94 (range 9.81–13.88) and 1.99 m ± 0.19 (range 1.49–2.40). Immature females ($n = 8$) displayed higher values for WL (10.42 m ± 0.94, range 8.44–11.56) and OW (1.78 m ± 0.17, range 1.42–1.92) when compared to immature males ($n = 9$) WL (9.70 m ± 0.84, range 8.30–10.75) and OW values (1.65 m ± 0.16, range 1.42–1.92). For calves ($n = 2$), the mean WL was 7.61 m ± 0.48 (range 7.27–7.95) and mean OW was 1.39 m ± 0.10 (range 1.31–1.46; Appendix S2: Fig. S2).

Absolute WL values in 2017 and 2018 and the strong correlation between WL and OW ($R^2 = 0.68$, slope = 0.16, $P < 0.001$; Appendix S2: Fig. S3) were comparable with data previously documented for gray whales (Perryman and Lynn 2002), with calves representing the smaller whales (<8 m). Yet, it is the residuals around the correlation line between WL and OW that describes the variation of individual body condition, which is captured through comparison of the BAI metric that relates the whale's SA between the 20% and 60% body length to WL.

Model selection

Ten linear mixed models were compared to assess the influence of multiple predictor variables on BAI (Table 3). Model 5 had the lowest AIC (AIC = 1306.06, df = 20), yet study site was not a significant variable ($P > 0.05$) in the model. Thus, model 4 was selected as the most parsimonious model because it did not include study site and only had a marginally lower AIC (LMM, AIC = 1307.74, df = 19, $R^2_m = 0.24$, $R^2_c = 0.37$). In model 4, demographic units ($F = 3.17$, $P < 0.01$, df = 10), month ($F = 5.46$, $P < 0.001$, df = 4), and year ($F = 13.56$, $P < 0.001$, df = 2) exhibited significant effects on BAI, where year was the most significant factor.

The generalized linear model describing the effects on CUI with the lowest AIC (AIC = 28960.22, df = 73, $R^2 = 0.55$; Appendix S2: Table S2) included the predictor variables month (GLM, $F = 153.90$, $P < 0.001$, df = 11), year (GLM, $F = 41.26$, $P < 0.001$, df = 5), and the

Table 2. Unmanned aerial system (UAS) overflights of gray whales by number of individuals (N_{ind}), number of observations (N_{obs}), and respective mean and standard deviation (SD, in parentheses) of BAI per demographic unit per year.

Demographic units	2016				2017				2018			
	N_{ind}	BAI	N_{obs}	BAI	N_{ind}	BAI	N_{obs}	BAI	N_{ind}	BAI	N_{obs}	BAI
Calf	3	44.61 (5.40)	3	44.61 (5.40)	1	41.33	1	41.33	1	41.89	1	41.9
Immature male	0	NA	0	NA	5	38.99 (2.68)	9	38.84 (2.33)	3	36.78 (1.87)	6	37.38 (1.82)
Immature female	5	40.11 (2.41)	5	40.11 (2.41)	5	38.67 (2.79)	8	38.38 (2.58)	4	37.37 (3.42)	9	37.92 (2.57)
Immature unknown sex	0	NA	0	NA	5	38.15 (2.27)	6	38.49 (2.49)	4	40.50 (0.71)	7	40.47 (1.16)
Mature male	15	40.80 (3.39)	21	40.77 (3.63)	13	38.93 (2.89)	22	38.9 (2.67)	16	38.14 (2.31)	33	38.24 (2.74)
Mature unknown sex	2	40.86 (4.54)	2	40.86 (4.54)	2	37.65 (1.08)	2	37.65 (1.08)	4	38.05 (1.78)	8	39.09 (2.31)
Resting female	14	41.19 (2.03)	23	41.21 (2.63)	12	38.23 (2.46)	28	38.51 (3.15)	13	38.21 (3.04)	26	38.4 (2.48)
Pregnant female	1	43.87	1	43.87	1	43.45	1	43.45	1	42.42	1	42.42
Lactating female	3	35.75 (2.84)	4	36.28 (2.60)	1	34.61	1	34.61	1	38.07	2	38.07 (2.26)
Postweaning female	1	38.32	2	38.32 (1.95)	1	36.37	2	36.38 (0.68)	1	38.11	2	38.11 (3.41)
Undetermined	11	40.20 (2.84)	16	40.21 (3.69)	9	37.83 (2.21)	13	37.7 (2.09)	6	39.64 (1.61)	7	39.85 (1.652)

Notes: The number of observations is relative to the number of different flights conducted over these individuals. Individual whales may be represented in this table multiple times in case of (1) sightings in multiple years, and/or (2) change in reproductive female cycle within a year. NA, not applicable.

interaction of month × year (GLM, $F = 12.24$, $P < 0.001$, df = 55).

Demographic unit comparisons

Gray whale BAI varied significantly relative to demographic units (Fig. 2). Calves displayed the highest mean BAI ($n = 5$; 43.41 ± 4.16 [mean ± SD]), followed by pregnant females ($n = 3$; 43.25 ± 0.75), resting females ($n = 26$; 39.41 ± 2.48), mature males ($n = 30$; 39.16 ± 2.51), immatures of unknown sex ($n = 8$; 39.00 ± 2.11), matures of unknown sex ($n = 6$; 38.94 ± 2.89), immature males ($n = 7$; 38.85 ± 2.62), immature females ($n = 6$; 38.29 ± 2.68), postweaning females ($n = 3$; 37.60 ± 1.07), and, finally, lactating females ($n = 5$; 35.99 ± 2.37), which presented the most depleted body condition. The high variation in female body condition between reproductive phases was also detectable at the individual level where BAI values fluctuated with repeated measurements of the same individual during different phases (e.g., Fig. 3). Furthermore, all ($n = 4$) but one lactating female examined in this study displayed a worse body condition in the year they were lactating (36.41 ± 2.15 [mean BAI ± SD]) compared to years when they were in resting (37.16 ± 4.71) or pregnant (43.66 ± 0.30) states. Also, all lactating females exhibited improved body condition after weaning events ($n = 3$; lactating females: 35.07 ± 2.80; postweaning females: 37.60 ± 1.06).

Table 3. Linear mixed model selection parameters of gray whale body area index (BAI) relative to the predictor variables demographic unit (DU), day of the year (DOY), month, year, and study site.

Models	df	AIC
(1) BAI ~ DU + (1|ID)	13	1349.597
(2) BAI ~ DU + month + (1|ID)	17	1329.607
(3) BAI ~ DU + year + (1|ID)	15	1322.546
(4) BAI ~ DU + month + year + (1|ID)	**19**	**1307.745**
(5) BAI ~ DU + month + year + study site + (1|ID)	20	1306.065
(6) BAI ~ study site + (1|ID)	4	1364.056
(7) BAI ~ DU + DOY + (1|ID)	14	1337.516
(8) BAI ~ DU + DOY + month + (1|ID)	18	1330.192
(9) BAI ~ DU + DOY + month + year + (1|ID)	20	1310.104
(10) BAI ~ DU + DOY + month + year + study site (1|ID)	21	1309.088

Notes: All models used whale identification (ID) as a random effect. Model 4 (in bold) was selected as the best and most parsimonious model based on the Akaike information criterion (AIC) and the insignificance of study site and DOY to the model.

Significant BAI differences were found between calves and immature females ($P < 0.05$), mature

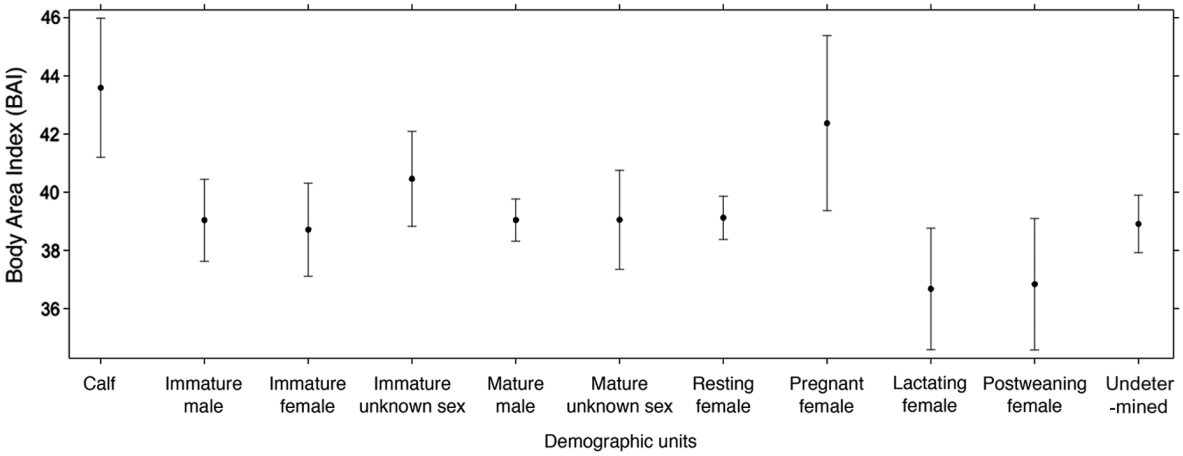

Fig. 2. The effect of demographic units on gray whale body area index (BAI) measured during June–October of 2016–2018 along the Oregon coast, USA, derived from linear mixed model results with whale identification as random effect (model 4).

males ($P < 0.05$), resting females ($P < 0.05$), lactating females ($P = 0.001$), postweaning females ($P < 0.01$), and undetermined ($P < 0.05$; Table 4).

Intra- and inter-annual body condition variation

BAI values calculated from raw pixel values and from scaled metric values had a perfect linear relationship ($r = 1$, $P = 0$), demonstrating that 2016 BAI values are comparable to 2017 and 2018 measurements despite a lack of accurate altitude values in 2016 to facilitate scaled metric measurements.

Gray whales exhibited an overall intra-annual improvement in body condition across the foraging season months, indicating energetic gain at the population level throughout the feeding seasons (Fig. 4A). However, the linear model results show a significant increase in body condition over the months in 2017 (rate of change = 0.03, $F_{1,88} = 15.7$, $P < 0.001$, $R^2 = 0.142$) and 2018 (rate of change = 0.01, $F_{1,96} = 6.302$, $P < 0.05$, $R^2 = 0.01$), while in 2016, improvement in body condition was nonsignificant (rate of change = 0.01, $F_{1,67} = 1.178$, $P > 0.05$, $R^2 = 0.003$).

Significant BAI differences were found between the months June and September ($P < 0.01$) and October ($P < 0.05$), and between July and September ($P < 0.01$) and October ($P < 0.05$; Table 4). Significant BAI differences were also found between the years 2016 and 2017 ($P < 0.001$) and between 2016 and 2018 ($P < 0.001$), but not between 2017 and 2018 (Table 4).

Gray whale body condition had significant inter-annual variation (Fig. 4B). The population presented the best body condition in 2016 ($n = 57$; 40.82 ± 2.91 [mean BAI $\pm$ SD]), followed by 2017 ($n = 55$; 38.67 ± 2.45) and 2018 ($n = 54$; 38.62 ± 2.38), when considering a mean per whale per demographic unit.

Upwelling index

Significant annual variation in the CUI was observed between the study years with the highest CUI levels occurring in 2015 and 2013, followed by 2014 and 2018 with values near the mean, and then, 2017 and 2016 had the lowest CUI levels, which were below the mean (Fig. 5). These data illustrate the relatively poor upwelling conditions in the study area from 2016 through 2018, particularly during 2016. All three years were significant predictors of CUI variation (2016, $F = -315.807$; 2017, $F = -422.073$; and 2018, $F = -582.113$; $P < 0.001$).

Assessment of the CUI for the 1993–1998 period that preceded the 1999–2000 gray whale mortality event indicates that three of the years (1993, 1995, and 1998) were below the mean during the foraging period (1 June–15 October; Appendix S2: Fig. S4). In contrast to the observed three-year period of relatively low CUI values

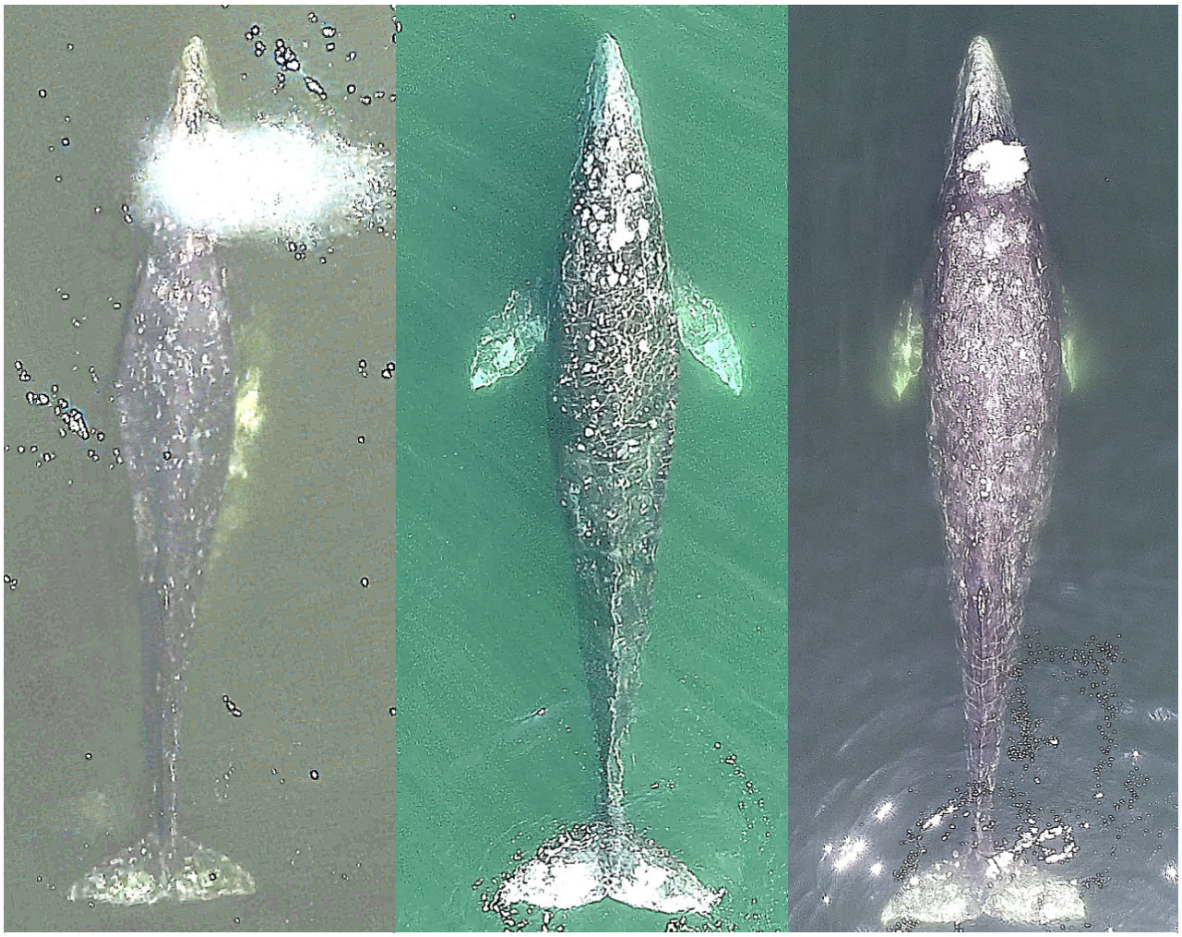

Fig. 3. Body condition comparison of a female whale over the years and throughout different reproductive states using the body area index (BAI) metric. Differences in image quality are associated with the drone used for overflights (June 2016, DJI Phantom 3 Pro; October 2016, DJI Phantom 4; and September 2018, DJI Phantom 4 Pro).

during the 2016–2018 period that preceded the 2019 gray whale mortality event, the three-year period of 1996–1998 that preceded the 1999–2000 mortality event did not display a similar low CUI trend.

Discussion

This study builds upon foundational studies of baleen whale body condition variation on foraging grounds (Lockyer 1986, Bradford et al. 2012) through application of quantitative drone-based photogrammetry metrics to describe gray whale body condition change over three consecutive feeding seasons relative to time, demographic unit, and environmental conditions. We document significant differences in whale body condition by month with general improvement as the foraging season progressed, by demographic unit with lactating females having the least fat reserves, and by year with potential links to temporally lagged environmental conditions. These findings demonstrate the utility of the BAI metric to detect and quantify variation in whale body condition at both the population level and individual level, which can be applied to monitor

Table 4. Significant pairwise comparison of estimated marginal means (EMMs) of the most parsimonious linear mixed model (model 4) for gray whale body area index (BAI) according to the variables demographic unit, month, and year.

Contrast	Estimate	SE	df	*T* ratio	*P*
Calf, immature female	4.88152	1.476	180.2	3.308	0.0436
Calf, mature male	4.54966	1.275	223.3	3.569	0.0186
Calf, resting female	4.47262	1.277	220.2	3.503	0.0231
Calf, lactating female	6.91745	1.591	231.8	4.347	0.0010
Calf, postweaning female	6.75570	1.688	233.5	4.002	0.0040
Calf, undetermined	4.68251	1.309	224.5	3.577	0.0181
June–September	−1.693	0.485	255	−3.492	0.0051
June–October	−1.739	0.615	255	−2.828	0.0401
July–September	−2.127	0.608	249	−3.501	0.0049
July–October	−2.173	0.701	252	−3.100	0.0182
2016–2017	2.0038	0.449	253	4.459	<0.0001
2016–2018	2.0296	0.432	254	4.693	<0.0001

baleen whale population health relative to environmental and anthropogenic perturbations.

The utility of BAI

We documented a perfect fit of BAI values between scaled and unscaled photogrammetry images. Therefore, despite unscaled images in 2016, we demonstrate that the unitless and scale-invariant BAI metric can still be confidently applied to assess whale body condition and allow comparisons across time periods when derived from measurements of low-distortion nadir images over relatively flat water. Hence, the BAI can be applied to many datasets of aerial whale images captured in nadir that lack accurate altitude data (e.g., from helicopters, airplanes, or drones) for robust assessment and comparison of body condition. We are confident that the BAI can add significant value to many historical aerial image datasets to foster exploration of pressing research questions regarding the impacts of environmental change on whale health. Additionally, while drone-based quantitative photogrammetry assessments of whale body condition, such as BAI, improve upon categorical determinations from oblique photographs (i.e., Bradford et al. 2012), the two methods can be (1) used to validate each other and (2) integrated to temporally extend assessment periods.

Intra-annual body condition variation by demographic unit

At the population level, gray whale body condition improved significantly across months with the progression of the feeding season in 2017 and 2018, indicating energy replenishment (Figs. 3, 4A). This result demonstrates that whales gain mass during the feeding season, and aligns with previous body condition assessments in fin, and western and eastern gray whales (Rice and Wolman 1971, Lockyer 1986, 1987*a*, Perryman and Lynn 2002, Bradford et al. 2012).

Interestingly, in 2016 when the whales were in relatively good body condition following at least three years of above-average upwelling conditions, whale body condition did not show a significant trend over months. Perhaps when whales are already robust and energetic requirements are satisfied, they reduce their energy intake rate, as has been postulated by Machovsky-Capuska and Raubenheimer (2020), gain mass more slowly, or have limited capacity to gain more mass. However, studies on this topic are scarce and a longer time series is needed to assess these ideas.

Gray whale body condition also varied according to sex, age, and reproductive status, with calves displaying the highest mean BAI, followed by pregnant females, while lactating and postweaning females had the lowest BAI values (Fig. 2). These results are consistent with previous findings reported for western gray whales (Bradford et al. 2012) and right whales (*Eubalaena australis* and *E. glacialis*; Angell 2006), yet et al. (2016) used drone-based photogrammetry to document that humpback whale (*Megaptera novaeangliae*) calves on a breeding ground exhibited the worst body condition index (BCI), followed by immature, mature, and lactating females. This contrast in relative calf body condition between studies may be due to the method of body condition assessment (BAI vs. BCI), where BCI is an absolute measure of body condition that does not account for the length of the animals. Furthermore, et al. (2016) investigated how whale body condition declined on breeding grounds over a two-month period, while the

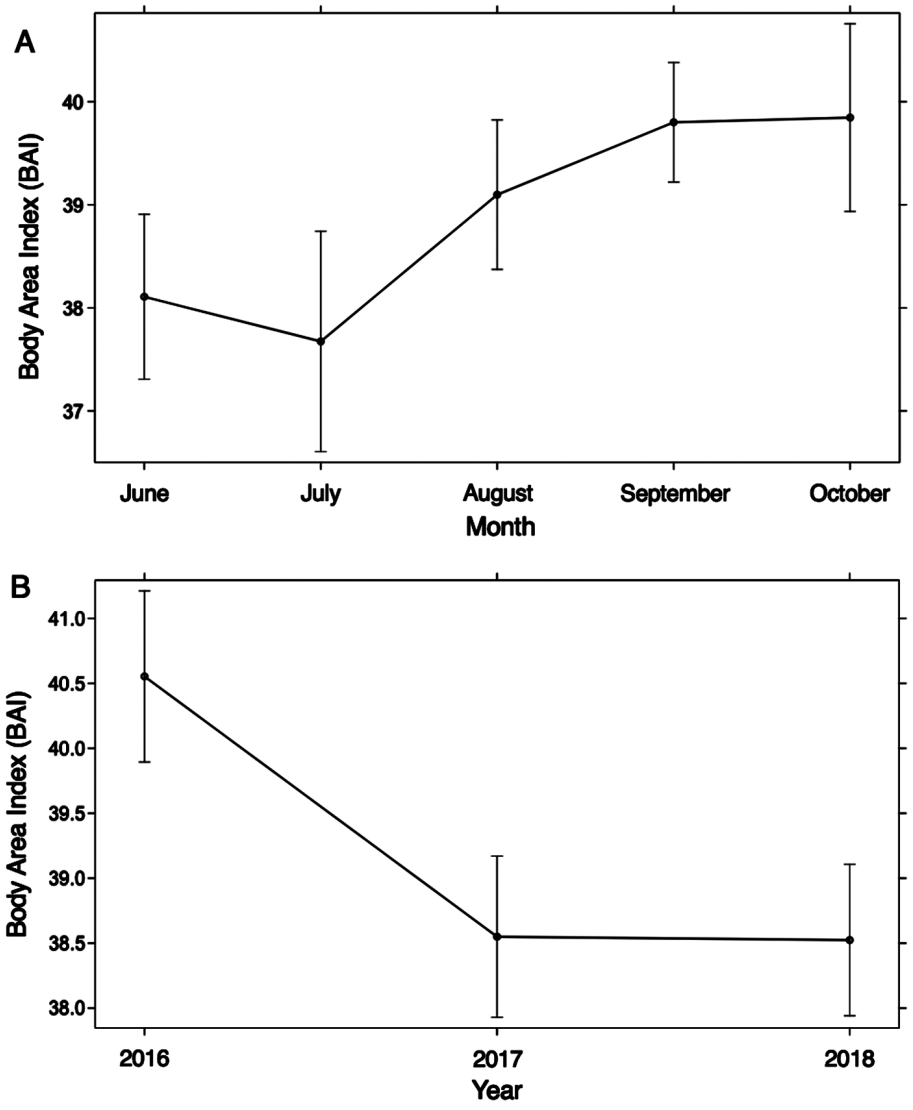

Fig. 4. Gray whale body area index (BAI), measured during June–October of 2016–2018 along the Oregon coast, USA, as a function of (A) month and (B) year, derived from linear mixed model results with whale identification as random effect (model 4). No sampling effort was performed in July 2016.

present study investigated the improvement of body condition on foraging grounds over five-month periods in three different years. Although our dataset contained no repeated photogrammetric data for any calf within a year, the high BAI values for all calf measures indicate that they were well nourished, reflecting the high milk fat transfer from mother to calf (Rice and Wolman 1971).

Our assessment of body condition by demographic unit also indicates that lactating females represent the most depleted group, while pregnant females represent one of the most robust groups on the foraging grounds, aligning well with previous studies (Lockyer 1987*a*, Perryman and Lynn 2002, Pettis et al. 2004, Miller et al. 2011, Bradford et al. 2012). Baleen whales are iteroparous with lactation considered the most energetically demanding phase of the female reproductive cycle (Lockyer 1981, Gittleman and Thompson 1988). Thus, it is crucial that pregnant females develop a significant energy storage

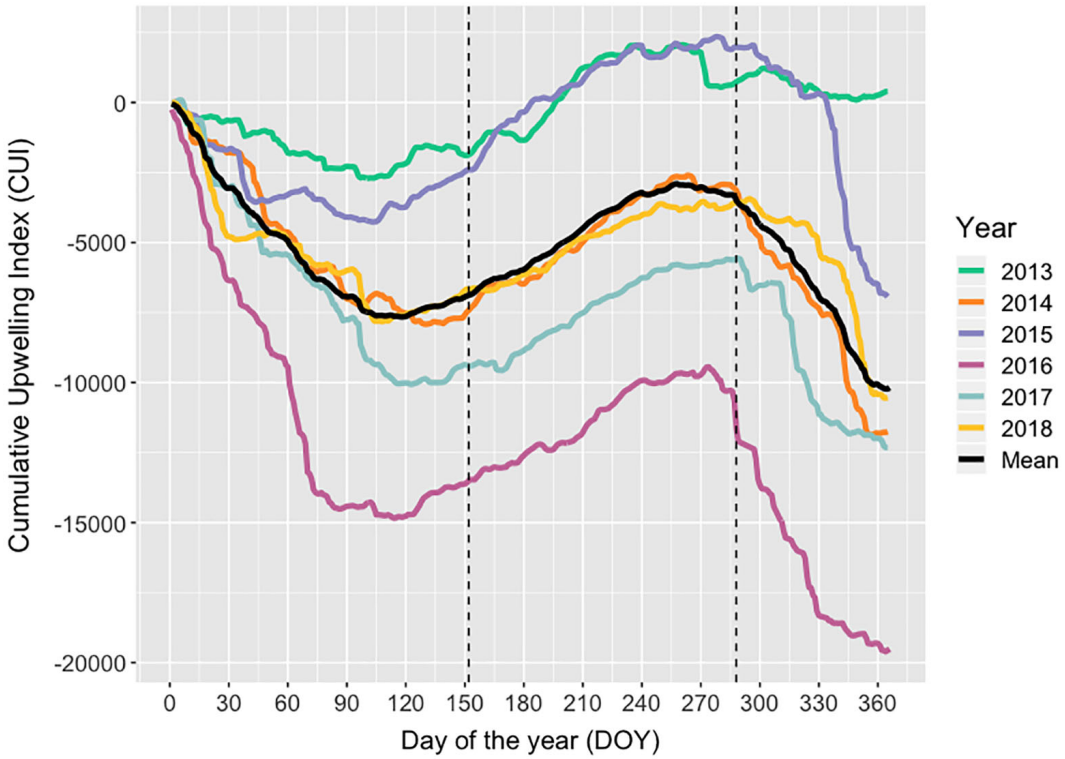

Fig. 5. Cumulative upwelling index (CUI; $m^3/s/100$ m coastline) computed from the daily upwelling index at the west coast of United States, offshore of Newport, Oregon (latitude 45° N, longitude − 125° W), from 2013 to 2018. The black line represents the cumulative sum of the daily means over the six years. The black dashed vertical lines mark the study period (1 June–15 October). Daily upwelling index data obtained from http://upwell.pfeg.noaa.gov/erddap/.

during the prior feeding season(s) to successfully gestate, birth, cover the high costs of lactation, and support her own metabolic needs (Lockyer 2007, et al. 2013, 2016). Interestingly, we observed nine mother–calf pairs in 2016, when the body condition was relatively good following multiple years of productive upwelling conditions. In contrast, we only observed one mother–calf pair in 2017 and one in 2018, when gray whale body condition was relatively poor. These findings indicate that prey resources in the previous years (2016 and 2017) may not have been sufficient for females to store adequate energy reserves to invest in reproduction in 2017 and 2018, which aligns with previous findings (Perryman et al. 2002).

We also document improved body condition of lactating females after weaning events, which is in line with previous findings (Miller et al. 2011) and highlights the importance of successful foraging seasons to allow reproductive females to recover. Variations in timing and extent of body condition improvement of postweaning mothers may be due to individual foraging and movement patterns, energetic transfer to calves, and environmental conditions that influence prey availability.

Inter-annual body condition variation associated with the upwelling index

PCFG gray whales exhibited a significantly better body condition in 2016 when compared to the following years, suggesting a lack of adequate prey availability and energy reposition by whales preceding measurement during the 2017 and 2018 seasons. This hypothesis is supported by our assessment of CUI from 2013 to 2018, which indicates the potential for carry-over effects between environmental conditions (used as a proxy for prey availability) and whale body

condition in subsequent feeding seasons. We assume that favorable upwelling conditions result in increased prey for whales in Oregon, based on (1) the strong links between upwelling in the CCS and increased primary production in the spring (Schroeder et al. 2009), and (2) shifts in the copepod zooplankton species toward communities lacking lipid content in Oregon during periods of reduced upwelling (Peterson et al. 2017). Although our analysis is limited to three years of gray whale body condition data relative to upwelling strength, an intriguing relationship is highlighted that requires further data collection and analysis to confirm or deny the correlation.

The one-year delay between the worst observed upwelling year in 2016 and evidence of poor gray whale body condition in 2017 is possibly due to carry-over effects of low prey quality or quantity conditions during the previous foraging season. Body condition potentially remained poor in 2018 due to cumulative carry-over effects of another low upwelling year in 2017. Such temporal lags between environmental conditions and whale biology have also been documented between the duration of the feeding season and the number of gray whale calves in the following year (Perryman et al. 2002), and between water temperature and southern right whale (*E. australis*) reproductive success (Leaper et al. 2006). The 2019 unusual mortality event of gray whales along the west coasts of Mexico, the United States, and Canada may also be related to the cumulative impacts of oceanographic conditions that reduce prey availability. Three consecutive years of relatively poor upwelling may indicate the limit of gray whale resilience to prey shortages; gray whales may be resilient to one or two years of poor prey conditions (e.g., 2016 and 2017), and reach an energetic reserve threshold after three years of reduced foraging success (e.g., 2016–2018), leading to high mortality rates due to emaciation. Indeed, upwelling conditions prior to the 1999–2000 mortality event were stronger than the recent period, although also variable. Hence, factors other than environmental fluctuations that influence prey availability may have been responsible for the previous mortality event, such as thresholds of population carrying capacity, as hypothesized by Rugh et al. (2005) and Coyle et al. (2007).

Disentangling the potential causes of the 2019 mortality event is challenging, as both limits of carrying capacity and unfavorable oceanographic conditions may be synergistic factors. While the qualitative correlation between CUI and gray whale body condition indicates the potential influence of upwelling strength in the region, several other oceanographic events occurred in parallel to the weak upwelling from 2016 to 2018, intensifying negative conditions (Appendix S2: Fig. S5). Starting in November 2013, anomalously warm conditions (event known as The Blob) were observed in the entire CCS, reaching its extreme in mid-2016 (Gentemann et al. 2017). In addition, the years 2015 and 2016 were characterized by the strongest El Niño ever recorded, which intensified sea surface temperatures and caused a drastic decline in primary productivity (Peterson et al. 2002, Durski et al. 2015, Di Lorenzo and Mantua 2016). A positive Pacific Decadal Oscillation (PDO) phase associated with reduced upwelling occurred during 2016 and 2017, peaking in April 2016 (Di Lorenzo et al. 2008, Thompson et al. 2018), and a negative phase of the North Pacific Gyre Oscillation (NPGO) was observed for almost the entire period from 2013 to 2018 (Di Lorenzo et al. 2008, Thompson et al. 2018). There is also evidence that copepod and krill communities were affected along the CCS during the same period (Thompson et al. 2018). Therefore, it is possible that mysid prey of gray whales along the Oregon coast were also negatively affected. The cumulative effects of these oceanographic features between 2013 and 2018 may have created prolonged non-nutritious feeding conditions in the CCS, causing depleted gray whale body condition in the later years of our study (2017 and 2018), and possibly contributed to the current mortality event.

Conclusions

This study demonstrates the utility of long-term photogrammetric monitoring of baleen whales on their foraging grounds. We document variability in gray whale body condition relative to month of the foraging season, demographic unit, and year. We also present correlative evidence to support the hypothesis that upwelling conditions may have a carry-over effect on gray

whale body condition in the following years. These findings help to fill knowledge gaps regarding how baleen whales recover from fasting periods or reproductive phases (pregnancy; lactation) and respond to environmental variation. Additionally, we place our results within the context of the 2019 gray whale unusual mortality event, illustrating the value of longitudinal assessment of whale body condition for population management. In addition, our methods can be extended to the majority of the ENP gray whale population that feed in the Alaskan Arctic to increase sample size, allow comparison by habitat and prey, and assess whale response to larger scale events, such as climate change. We recommend continued monitoring of gray whale body condition to better understand the causes of nutrition-limited mortality events, and the subsequent consequences and recovery of this population. Furthermore, we show that BAI is robust to scaling errors and can be applied to aerial whale image datasets that lack scale and altitude data, such as our 2016 dataset or archived aerial image datasets from helicopters, enabling valuable comparisons of whale health across time periods and populations to inform conservation efforts.

Acknowledgments

This research was funded by the NOAA National Marine Fisheries Service Office of Science and Technology Ocean Acoustics Program, Oregon Sea Grant Program Development funds, and the Oregon State University (OSU) Marine Mammal Institute. We are thankful for the support of Brazil's Science Without Borders Program, Brazil's CNPq, the Harvard Laspau Institute, and the Mamie Markham Research Award (Hatfield Marine Science Center/OSU), which provided financial aid and support for LSL. We are grateful to research assistants Danielle Marie Balderson and Taylor Mock for assistance with photogrammetry analysis, Joseph D. Maurer (Statistics Department/OSU), Lucas Kopecky Bobadilla (OSU) and Mariana Bonfim (Temple University) for statistical support, Isaac Schroeder (Southwest Fisheries Science Center/NOAA) for advice on upwelling index analysis, John Calambokidis and Alie Perez at the Cascadia Research Collective for assistance with the photo-identification analysis, and Debbie Steel and Scott Baker (OSU) for assistance with genetic analyses. We are extremely grateful to Amanda Bradford and other anonymous reviewer for insightful comments that improved this manuscript. This research was conducted under NOAA/NMFS permits #16011 and #21678 issued to John Calambokidis. Publication of this paper was supported, in part, by the Henry Mastin Graduate Student Fund.

Literature Cited

Acevedo-Whitehouse, K., and A. L. J. Duffus. 2009. Effects of environmental change on wildlife health. Philosophical Transactions of the Royal Society B: Biological Sciences 364:3429–3438.

Angell, C. M. 2006. Body fat condition of free-ranging right whales, *Eubalaena glacialis* and *Eubalaena australis*. Dissertation. Boston University, Boston, Massachusetts, USA.

Barto, K. 2018. MuMIn: multi-model inference. R package version 1404. https://cran.r-project.org/package=MuMIn

Bates, D., M. Maechler, B. Bolker, and S. Walker. 2015. Fitting linear mixed-effects models using lme4. Journal of Statistical Software 67:1–48.

Benoit-Bird, K. J., and M. A. McManus. 2012. Bottom-up regulation of a pelagic community through spatial aggregations. Biology Letters 8:813–816.

Best, P. B., and H. Ruther. 1992. Aerial photogrammetry of southern right whales, *Eubalaena australis*. Journal of Zoology 228:595–614.

Bograd, S. J., I. Schroeder, N. Sarkar, X. Qiu, W. J. Sydeman, and F. B. Schwing. 2009. Phenology of coastal upwelling in the California Current. Geophysical Research Letters 36:1–5.

Bradford, A. L., D. W. Weller, A. E. Punt, Y. V. Ivashchenko, A. M. Burdin, G. R. VanBlaricom, and R. L. Brownell. 2012. Leaner leviathans: body condition variation in a critically endangered whale population. Journal of Mammalogy 93:251–266.

Braithwaite, J. E., J. J. Meeuwig, and M. R. Hipsey. 2015*a*. Optimal migration energetics of humpback whales and the implications of disturbance. Conservation Physiology 3:1–15.

Braithwaite, J. E., J. J. Meeuwig, T. B. Letessier, K. C. S. Jenner, and A. S. Brierley. 2015*b*. From sea ice to blubber: linking whale condition to krill abundance using historical whaling records. Polar Biology 38:1195–1202.

Burnett, J., L. S. Lemos, D. Barlow, M. Wing, T. Chandler, and L. Torres. 2018. Estimating morphometric attributes of baleen whales with photogrammetry from small UAS: a case study with blue and gray whales. Marine Mammal Science 35:108–139.

Burnham, K. P., D. R. Anderson, and K. P. Huyvaert. 2011. AIC model selection and multimodel inference in behavioral ecology: some background, observations, and comparisons. Behavioral Ecology and Sociobiology 65:23–35.

Calambokidis, J., et al. 2002. Abundance, range and movements of a feeding aggregation of gray whales (*Eschrichtius robustus*) from California to southeastern Alaska in 1998. Journal of Cetacean Research and Management 4:267–276.

Calambokidis, J., J. L. Laake, and A. Klimek. 2012. Updated analysis of abundance and population structure of seasonal gray whales in the Pacific Northwest, 1998–2010. International Whaling Commission, Cambridge, UK.

Christiansen, F., A. M. Dujon, K. R. Sprogis, J. P. Y. Arnould, and L. Bejder. 2016. Noninvasive unmanned aerial vehicle provides estimates of the energetic cost of reproduction in humpback whales. Ecosphere 7:e01468.

Christiansen, F., G. A. Vikingsson, M. H. Rasmussen, and D. Lusseau. 2013. Minke whales maximise energy storage on their feeding grounds. Journal of Experimental Biology 216:427–436.

Christiansen, F., F. Vivier, C. Charlton, R. Ward, A. Amerson, S. Burnell, and L. Bejder 2018. Maternal body size and condition determine calf growth rates in southern right whales. Marine Ecology Progress Series 592:267–281.

Coyle, K. O., B. Bluhm, B. Konar, A. Blanchard, and R. C. Highsmith. 2007. Amphipod prey of gray whales in the northern Bering Sea: comparison of biomass and distribution between the 1980s and 2002–2003. Deep-Sea Research II 54:2906–2918.

Cury, P. M., Y.-J. Shin, B. Planque, J. M. Durant, J.-M. Fromentin, S. Kramer-Schadt, N. C. Stenseth, M. Travers, and V. Grimm. 2008. Ecosystem oceanography for global change in fisheries. Trends in Ecology and Evolution 23:338–346.

Darling, J. D. 1984. Gray whales off Vancouver Island, British Columbia. Pages 267–287 *in* M. L. Jones, S. L. Swartz, and S. Leatherwood, editors. The gray whale *Eschrichtius robustus*. Academic Press, Orlando, Florida, USA.

Di Lorenzo, E., et al. 2008. North Pacific Gyre Oscillation links ocean climate and ecosystem change. Geophysical Research Letters 35:1–6.

Di Lorenzo, E., and N. Mantua. 2016. Multi-year persistence of the 2014/15 North Pacific marine heatwave. Nature Climate Change 6:1042–1048.

Durban, J. W., M. J. Moore, G. Chiang, L. S. Hickmott, A. Bocconcelli, G. Howes, P. A. Bahamonde, W. L. Perryman, and D. J. LeRoi. 2016. Photogrammetry of blue whales with an unmanned hexacopter. Marine Mammal Science 32:1510–1515.

Durski, S. M., A. L. Kurapov, J. S. Allen, P. M. Kosro, G. D. Egbert, K. Shearman, and J. A. Barth. 2015. Coastal ocean variability in the US Pacific Northwest region: seasonal patterns, winter circulation, and the influence of the 2009–2010 El Niño. Ocean Dynamics 65:1643–1663.

Gallagher, D., M. Visser, D. Sepulveda, R. N. Pierson, T. Harris, and S. B. Heymsfield. 1996. How useful is body mass index for comparison of body fatness across age, sex, and ethnic groups. American Journal of Epidemiology 143:228–239.

Gentemann, C. L., M. R. Fewings, and M. García-Reyes. 2017. Satellite sea surface temperatures along the West Coast of the United States during the 2014–2016 northeast Pacific marine heat wave. Geophysical Research Letters 44:312–319.

Gittleman, J. L., and S. D. Thompson. 1988. Energy allocation in mammalian reproduction. American Zoologist 28:863–875.

Hammond, P. S., S. A. Mizroch, and G. P. Donovan. 1990. Individual recognition of cetaceans: use of photo-identification and other techniques to estimate population parameters. International Whaling Commission, Cambridge, UK.

Harrison, X. A., J. D. Blount, R. Inger, D. R. Norris, and S. Bearhop. 2011. Carry-over effects as drivers of fitness differences in animals. Journal of Animal Ecology 80:4–18.

Harvey, C., et al. 2018. Ecosystem Status Report of the California Current for 2018: a Summary of Ecosystem Indicators Compiled by the California Current Integrated Ecosystem Assessment Team (CCIEA). NOAA Fisheries, Northwest Fisheries Science Center, Seattle, Washington, USA.

Heymans, J. J., M. Coll, S. Libralato, L. Morissette, and V. Christensen. 2014. Global Patterns in ecological indicators of marine food webs: a modelling approach. PLOS ONE 9:e95845.

Hunter, T. C. R. 1978. The importance of a relative shortage of food in animal ecology. Oecologia 33:71–86.

Jones, M. L., and S. L. Swartz. 2002. Gray Whale, Eschrichtius robustus. Pages 524–536 *In* Encyclopedia of marine mammals. Academic Press, San Diego, California, USA.

Kasuya, T. 1995. Overview of cetacean life histories: an essay in their evolution. Pages 481–498 *in* A. S. Blix, L. Walløe and Ø. Ulltang, editors. Whales, seals, fish and man. Elsevier Science, Amsterdam, The Netherlands.

Koopman, H. N. 1998. Topographical distribution of the blubber of harbor porpoises (*Phocoena phocoena*). Journal of Mammalogy 79:260–270.

Kuznetsova, A., P. B. Brockhoff, and R. H. B. Christensen 2017. LmerTest package: tests in linear mixed effects models. Journal of Statistical Software 82:1–26.

Lang, A. R., J. Calambokidis, J. Scordino, V. L. Pease, A. Klimek, V. N. Burkanov, P. Gearin, D. I. Litovka, K. M. Robertson, B. R. Mate, J. K. Jacobsen, and B. L. Taylor.

2014. Assessment of genetic structure among eastern North Pacific gray whales on their feeding grounds. Marine Mammal Science 30:1473–1493.

Le Boeuf, B. J., H. Pérez-Cortés, J. Urbán, B. R. Mate, and F. Ollervides. 2000. High gray whale mortality and low recruitment in 1999: potential causes and implications. Journal of Cetacean Research and Management 2:85–99.

Leaper, R., J. Cooke, P. Trathan, K. Reid, V. Rowntree, and R. Payne. 2006. Global climate drives southern right whale (*Eubalaena australis*) population dynamics. Biology Letters 2:289–292.

Lenth, R. 2019. emmeans: estimated Marginal Means, aka Least-Squares Means. R package version 1.1.3. https://cran.r-project.org/package=emmeans

Lockyer, C. 1981. Estimation of the energy costs of growth, maintenance and reproduction in the female minke whale, (*Balaenoptera acutorostrata*), from the Southern Hemisphere. Report of the International Whaling Commission 31:337–343.

Lockyer, C. 1986. Body fat condition in northeast at antic Fin whales, *Balaenoptera physalus*, and its relationship with reproduction and food resource. Canadian Journal of Fisheries and Aquatic Sciences 43:142–147.

Lockyer, C. 1987*a*. Evaluation of the role of fat reserves in relation to the ecology of North Atlantic fin and sei whales. Pages 183–203 *in* A. C. Huntley, D. P. Costa, G. A. J. Worthy and M. A. Castellini, editors. Approaches to marine mammal energetics. Society for Marine Mammalogy, Lawrence, Kansas, USA.

Lockyer, C. 1987*b*. The relationship between body fat, food resource and reproductive energy costs in north Atlantic fin whales (*Balaenoptera physalus*). Symposia of the Zoological Society of London 57:343–361.

Lockyer, C. 2007. All creatures great and smaller: a study in cetacean life history energetics. Journal of the Marine Biological Association of the United Kingdom 87:1035–1045.

Machovsky-Capuska, G. E., and D. Raubenheimer. 2020. The nutritional ecology of marine apex predators. Annual Review of Marine Science 12:361–387.

Miller, C. A., P. B. Best, W. L. Perryman, M. F. Baumgartner, and M. J. Moore. 2012. Body shape changes associated with reproductive status, nutritive condition and growth in right whales *Eubalaena glacialis* and *E. australis*. Marine Ecology Progress Series 459:135–156.

Miller, C. A., D. Reeb, P. B. Best, A. R. Knowlton, M. W. Brown, and M. J. Moore. 2011. Blubber thickness in right whales *Eubalaena glacialis* and *Eubalaena australis* related with reproduction, life history status and prey abundance. Marine Ecology Progress Series 438:267–283.

Mooers, C. N. K., C. A. Collins, and R. L. Smith. 1976. The dynamic structure of the frontal zone in the coastal upwelling region off Oregon. Journal of Physical Oceanography 6:3–21.

Moore, S. E., J. Urban, W. L. Perryman, F. Gulland, H. Perez-Cortes, P. R. Wade, L. Rojas-Bracho, and T. Rowles. 2001. Are gray whales hitting "K" hard? Marine Mammal Science 17:954–958.

Nakagawa, S., and H. Schielzeth. 2013. A general and simple method for obtaining R^2 from generalized linear mixed effects models. Methods in Ecology and Evolution 4:133–142.

National Academies of Sciences, Engineering, and Medicine. 2017. Approaches to understanding the cumulative effects of stressors on marine mammals. The National Academies Press, Washington, D.C., USA.

Nattrass, S., and D. Lusseau. 2016. Using resilience to predict the effects of disturbance. Scientific Reports 6:25539.

New, L. F., D. J. Moretti, S. K. Hooker, D. P. Costa, and S. E. Simmons. 2013. Using energetic models to investigate the survival and reproduction of beaked whales (family *Ziphiidae*). PLOS ONE 8:e68725.

Newell, C. L., and T. J. Cowles. 2006. Unusual gray whale *Eschrichtius robustus* feeding in the summer of 2005 off the central Oregon Coast. Geophysical Research Letters 33:1–5.

NOAA. 2019. 2019 Gray Whale Unusual Mortality Event along the West Coast. Marine life in distress. https://www.fisheries.noaa.gov/national/marine-life-distress/2019-gray-whale-unusual-mortality-event-along-west-coast

Perryman, W. L., M. A. Donahue, P. C. Perkins, and S. B. Reilly. 2002. Gray whale calf production 1994–2000: Are observed fluctuations related to changes in seasonal ice cover? Marine Mammal Science 18:121–144.

Perryman, W. L., and M. S. Lynn. 2002. Evaluation of nutritive condition and reproductive status of migrating gray whales (*Eschrichtius robustus*) based on analysis of photogrammetric data. Journal of Cetacean Research and Management 4:155–164.

Peterson, W. T., J. L. Fisher, C. A. Morgan, S. M. Zeman, B. J. Burke, and K. C. Jacobson. 2018. Ocean ecosystem indicators of salmon marine survival in the northern California current. NOAA Fisheries, Northwest Fisheries Science Center, Seattle, Washington, USA.

Peterson, W. T., J. L. Fisher, P. T. Strub, X. Du, C. Risien, J. Peterson, and C. T. Shaw. 2017. The pelagic ecosystem in the Northern California current off Oregon during the 2014–2016 warm anomalies within the context of the past 20 years. Journal of Geophysical Research: Oceans 122:7267–7290.

Peterson, W. T., J. E. Keister, and L. R. Feinberg. 2002. The effects of the 1997–99 El Niño/La Niña events on hydrography and zooplankton off the central Oregon coast. Progress in Oceanography 54:381–398.

Pettis, H. M., R. M. Rolland, P. K. Hamilton, S. Brault, A. R. Knowlton, and S. D. Kraus. 2004. Visual health assessment of North Atlantic right whales (*Eubalaena glacialis*) using photographs. Canadian Journal of Zoology 82:8–19.

Pettis, H. M., R. M. Rolland, P. K. Hamilton, A. R. Knowlton, E. A. Burgess, and S. D. Kraus. 2017. Body condition changes arising from natural factors and fishing gear entanglements in North Atlantic right whales *Eubalaena glacialis*. Endangered Species Research 32:237–249.

R Core Team. 2019. R: a language and environment for statistical computing. R Foundation for Statistical Computing, Vienna, Austria.

Rice, D. W., and A. A. Wolman. 1971. The life history and ecology of the gray whale (*Eschrichtius robustus*). American Society of Mammalogists Special Publications 3:1–142.

Rugh, D. J., R. C. Hobbs, J. A. Lerczak, and J. M. Breiwick. 2005. Estimates of abundance of the eastern North Pacific stock of gray whales (*Eschrichtius robustus*) 1997–2002. Journal of Cetacean Research and Management 7:1–12.

Schroeder, I. D., W. J. Sydeman, N. Sarkar, S. A. Thompson, S. J. Bograd, and F. B. Schwing. 2009. Winter pre-conditioning of seabird phenology in the California current. Marine Ecology Progress Series 393:211–233.

Seyboth, E., K. R. Groch, L. D. Rosa, K. Reid, P. A. C. Flores, and E. R. Secchi. 2016. Southern right whale (*Eubalaena australis*) reproductive success is influenced by krill (*Euphausia superba*) density and climate. Scientific Reports 6:28205.

Sinclair, A. R. E., and C. J. Krebs. 2002. Complex numerical responses to top-down and bottom-up processes in vertebrate populations. Philosophical Transactions of the Royal Society of London. Series B: Biological Sciences 357:1221–1231.

Smith, C. E., S. T. Sykora-Bodie, B. Bloodworth, S. M. Pack, T. R. Spradlin, and N. R. LeBoeuf. 2016. Assessment of known impacts of unmanned aerial systems (UAS) on marine mammals: data gaps and recommendations for researchers in the United States. Journal of Unmanned Vehicle Systems 4:1–14.

Sumich, J. L. 2014. *E. robustus*: the biology and human history of gray whales. Whale Cove Marine Education, Corvallis, Oregon, USA.

Thomas, V. G. 1990. Control of reproduction in animal species with high and low body fat reserves. Pages 27–41 *in* R. E. Frisch, editor. Adipose tissue and reproduction (Progress in reproductive biology and medicine). S. Karger, Basel, Switzerland.

Thompson, A. R., et al. 2018. State of the California Current 2017–18: still not quite normal in the north and getting interesting in the south. CalCOFI Reports 59:1–66.

Tollefson, T. N., L. A. Shipley, W. L. Myers, D. H. Keisler, and N. Dasgupta. 2010. Influence of summer and autumn nutrition on body condition and reproduction in lactating mule deer. Journal of Wildlife Management 74:974–986.

Villegas-Amtmann, S., L. K. Schwarz, J. L. Sumich, and D. P. Costa. 2015. A bioenergetics model to evaluate demographic consequences of disturbance in marine mammals applied to gray whales. Ecosphere 6:1–19.

Weller, D. W., S. Bettridge, R. L. Jr Brownell, J. L. Laake, J. E. Moore, P. E. Rosel, B. L. Taylor, and P. R. Wade. 2013. Report of the National Marine Fisheries Service gray whale stock identification workshop. U.S. Department of Commerce, San Diego, California, USA.

Williams, R., G. A. Vikingsson, A. Gislason, C. Lockyer, L. New, L. Thomas, and P. S. Hammond. 2013. Evidence for density-dependent changes in body condition and pregnancy rate of North Atlantic fin whales over four decades of varying environmental conditions. ICES Journal of Marine Science 70:1273–1280.

Zimushko, V. V. 1969. Some data on the biology of gray whales. Pages 93–97 *in* V. A. Arseniev, B. A. Zenkovich, and K. K. Chapskii editors. Marine Mammals. Akademii Nauk, Moscow, Russia.

Zimushko, V. V., and M. V. Ivashin. 1980. Some results of U.S.S.R. investigations and whaling of gray whales (*Eschrichtius robustus*, Lilljeborg 1861). Report of the International Whaling Commission 30:237–246.

Supporting Information

Additional Supporting Information may be found online at: http://onlinelibrary.wiley.com/doi/10.1002/ecs2.3094/full